ISSN: 2277-3754
ISO 9001:2008 Certified
International Journal of Engineering and Innovative Technology (IJEIT)
Volume 4, Issue 3, September 2014

Activating Robotics Manipulator using Eye Movements

Eli Kolberg, Raphi Amsalem

Abstract*— The desire to help disabled people become more independent and satisfied led to study efforts in various fields. In particular this paper deals with helping severe injured disabled people that even simple tasks as moving objects from one place to the other is impossible for them. We will describe a novel approach for analyzing eye movement physiological signals that enables remote operation of a robotics manipulator. When eyeball movement is made, electric potentials are generated across the Cornea and Retina of the eyes within the conductive environment of the skull (Cornea-Retina Potential – CRP). It is the source of the Electro-Oculogram (EOG) signal. Using a differential amplifier followed by LPF filtration as described in the literature did not fit our goal to be able to filter the EOG signal even with interference of laughter or head move or other muscles action in the area of the head. We present a new approach that uses an additional specific band pass filter in order to create a robust system. The results show success in creating robust system that is capable of detecting eye movements in noisy environment and turn them into commands for a robotics manipulator.

***Index Terms*—aid tools for disabled, bio-engineering, eye movements detection, EOG signal.**

I. INTRODUCATION

Severe disabled people suffer from extreme paralysis that can result from reasons like brain injury or neurological diseases. National Multiple Sclerosis (MS) [1] and [2], estimate that world-wide, MS affects about 2.5 million people. According to The National Institute of Neurological Disorders and Stroke [3], as many as 20,000 Americans have Amyotrophic Lateral Sclerosis (ALS), and an estimated 5,000 people in the United States are diagnosed with the disease each year. ALS is one of the most common neuromuscular diseases worldwide, and people of all races and ethnic backgrounds are affected. ALS most commonly strikes people between 40 and 60 years of age, but younger and older people also can develop the disease. Men are affected more often than women. For severe disabled people, communication abilities are highly limited. In this paper we describe a method that makes the communication possible with low cost equipment and help the patient to activate a robotic manipulator with eye-movement only. Methods to detect eye-movement and gaze tracking involve either infra-red illumination as presented in [4] and [5] or high resolution camera as presented in [6] and [7]. Some works relates to use of low resolution camera as in [8]. The method we used is based on the Electro-ocular gram (EOG) signal for determining the position of the pupil of the eye. EOG signal is generated by dipoles located in the eyes with the cornea having relatively positive potential with respect to the retina as a result of the movement of eyeballs within the conductive environment of the skull [9]. The dipole voltage amplitude is about 1mV and frequency of 0.1Hz to 38 Hz [10, 11]. Movement of the eye generates a DC shift in the EOG voltage [11]. Within 30 degrees right or left in the horizontal axis (between the outer side of each eye), the change in the signal amplitude is linear relatively to the eye movement with a resolution of 2-20 micro-volts. Beyond 30 degrees it becomes nonlinear. Vertical axis measurements are less accurate and less reliable. There is a substantial electrical noise that comes with the EOG signal due to among others, physiological signals like EEG (stem from brain activity), and EMG (stem from muscles activity) [11]. The measurements described in this paper are of the horizontal axis. The measurement outcomes were sent by wireless communication devices to a robotic manipulator, which acted according to the input signal.

The system was robust and operated in various environments smoothly.

II. METHOD

A. Setup and Apparatus

The EOG based system for aid to disabled people consists of five parts: Amplification and filtering of the EOG signal, sampling the outcome signal, digital processing of the signal, transmitting the signal to a manipulator controller and activating the manipulator. The horizontal EOG signal measured as a voltage by means of electrodes strategically placed in the temple areas, close to each eye canthus. Each electrode measures the horizontal EOG with respect to a reference electrode placed on the center of the brow (see figure 1).

Fig 1: Electrode placement used to measure the horizontal EOG

Typical clean EOG signal has positive peak for eye movement to the left and negative peak for eye movement to the right [9]. Peak amplitudes are about 500 μV and duration of about 200ms. The hardware used included 1. AD instrument BIO-AMP testing instrument, which derive the analog EOG signals. It includes three components: Bio-Amp instrument with electrodes connected to it, POWERlab instrument that stands between the Bio-Amp and the

ISSN: 2277-3754
ISO 9001:2008 Certified
International Journal of Engineering and Innovative Technology (IJEIT)
Volume 4, Issue 3, September 2014

computer program, and LABchart software for determining the various parameters value for signal processing and signal view, 2. TI ADS8410/13 REF A/D with controlled sampling rate of up to 200MHz, 3. Xilinx Spartan3 XC3S400-FG456, 4. Parani BlueTooth communication components, and 5. a robotic manipulator system.

B. Software and User Interface

The system analyzed horizontal eye movements to right and left sides. The EOG signals received by the software were coded to commands with three symbols for each command. The symbols were "right", "left", and "center". The left movement defined as the digit '0', the right movement was defined as the digit '1', and "center" served as a control signal. The algorithm included: 1. Open the general display, 2. Calibrate the system with specific user (only for first time), 3. Display detailed instructions and a menu for manipulator commands, 4. Receive the user movement succession, including canceling specific movement and problems identification, 5. Approvie/deny of the incoming movement succession, 6. Send the proper command to the manipulator controller. A detailed algorithm for receive the user movement succession is presented in figure 2.

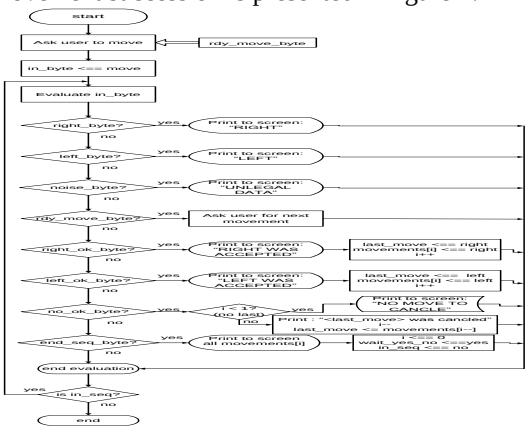

Fig 2: User movement succession receiving algorithm

III. PROCESSING THE MEASURED SIGNAL

EOG signal is usually accompanied with noise stem from environment signals and biological signals like EEG and EMG. The literature (e.g. [10], [11]), describe a two stages process for producing the signal. First stage includes amplifying the signal by a differential amplifier and the second stage includes filtering the signal by low pass filter with cutoff frequency of 38Hz. The first stage differential amplifier inputs are the signals received from right and left eyes. It should reject the common signal for the two inputs (noise) and amplify the difference between the two signals [10]. The purpose of the following stage, which is low pass filter, is to filter out the environmental noise. When we tested the system we discovered that whereas the signal is reasonable when no other muscle besides the eyes move, it is noisy and unpredictable when any other muscle is active, like with laughter, moving the head, etc. In addition, we discovered that in contrast to the description that the voltage is a function of the position of the eye, that when the eye move to a new position, the voltage becomes zero few milliseconds after the eye settles in a new position. In order to design a better solution for the system we started to sample the signals using LABchart with a frequency of 1KHz. Figure 3 presents a clean signal of left, center, right eye movement. Figure 4 presents noisy EOG signal.

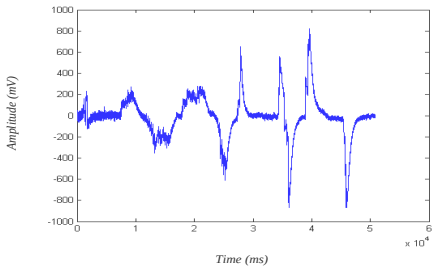

Fig 3: clean EOG signal

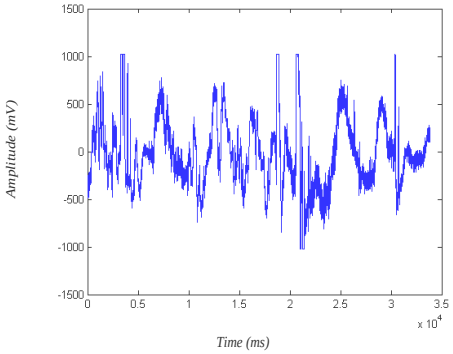

Fig 4: EOG signal with noise

It can be seen from figures 3 and 4 that most of the time, the values in the clean and noisy signals have the same scope. Thus, the band pass filter does not allow for separation in time (i.e. values in a specific range will be considered as clean signal and values outside this range will be considered as noise). Then we anticipated getting frequency range, in which only one type of signal will be present, in the frequency domain. We used the MatLab fft function for that purpose. Figure 5 presents the spectrum of the clean signal and figure 6 presents the spectrum of the noisy signal.

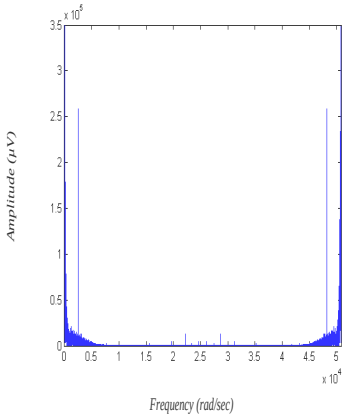

Fig 5: The spectrum of the clean signal

ISSN: 2277-3754
ISO 9001:2008 Certified
International Journal of Engineering and Innovative Technology (IJEIT)
Volume 4, Issue 3, September 2014

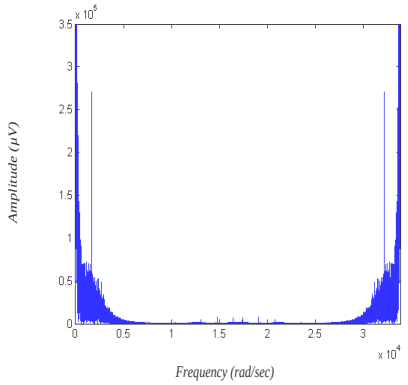

Fig 6: The spectrum of the noisy signal

A close look into the pictures shows that the signals are not bounded to specific frequencies, and the frequencies that look to be zero in this resolution are in fact non zero as can be seen in figures 7 and 8.

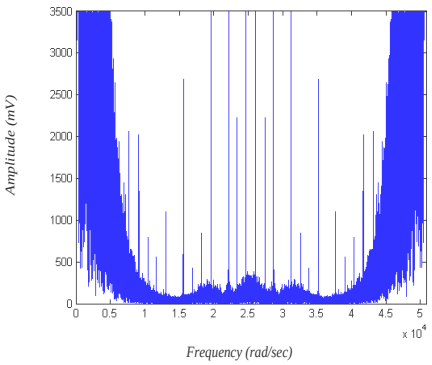

Fig 7: Close up of the clean signal spectrum

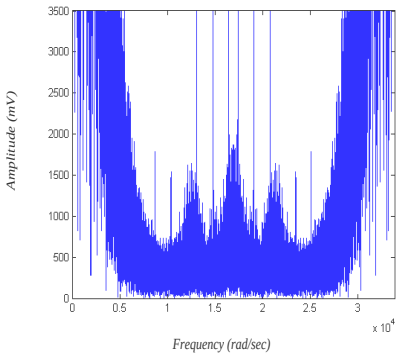

Fig 8: Close-up of the noisy signal spectrum

From these figures we can conclude that: 1. There is no frequency range in which only one signal type exists. 2. LPF filtering as suggested in the literature is not adequate here when muscle movements occur. 3. The 'peaks' we find in the spectrum of the two original signals (the 1695 sample in the noisy signal dft) is the environmental noise frequency (50Hz) found in the literature. We will prove that. The dft samples are the DTFT of the discrete signal in frequencies of (2Π/N)k where k=0…N-1. In our case N=33850 and k=1695. That makes the sampled frequency to be 2Π*0.050. The relation between the continuous frequency spectrum and the samples spectrum is given by Eq. 1.

$$X^{f}(\theta) = f_s \sum_{l=-\infty}^{\infty} X^{F}((\theta - 2\pi l) f_s)$$

(1)

When f_s is the sample frequency, X^{f} is the sample spectrum, and X^{F} is the continuous spectrum, in this case f_s = 1KHz.

Substituting the values:

$$X^{f}(2\pi * 0.050) = f_s X(2\pi * 0.050 * 1000) = 1k * X(2\pi * 50)$$

give sample frequency of 50Hz in the continuous spectrum multiplied by 1000.

4. For certain frequencies the spectrum amplitudes are significantly different between the two signals. In the noisy signal it is higher. The amplitude difference of the frequencies in the range of 60Hz to 80Hz (frequency range higher than the peak) seems to be the most significant.

IV. FILTERING THE EOG SIGNAL OF BIO-AMP TESTING

According to that we created a band pass filter. Figures 9 and 10 present the amplitude of the clean and noisy signals' spectrum after filtering respectively. Figures 11 and 12 present the amplitude of the clean and noisy signals respectively after filtering in the time domain.

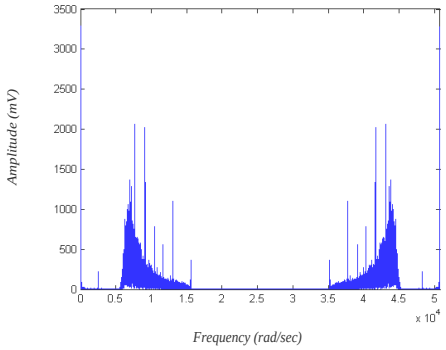

Fig 9: Clean signal spectrum after filtering

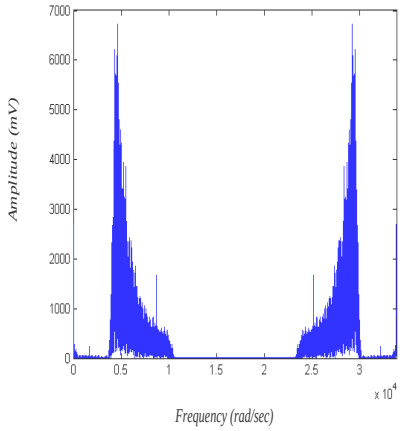

Fig 10: Noisy signal spectrum after filtering

ISSN: 2277-3754
ISO 9001:2008 Certified
International Journal of Engineering and Innovative Technology (IJEIT)
Volume 4, Issue 3, September 2014

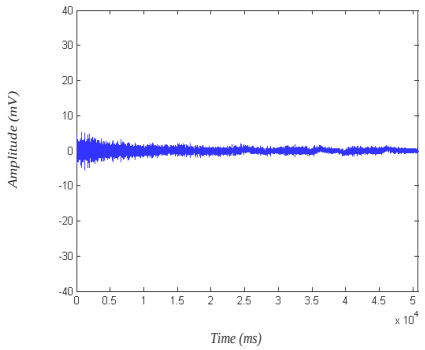

Fig 11: Clean signal spectrum after filtering in the time domain

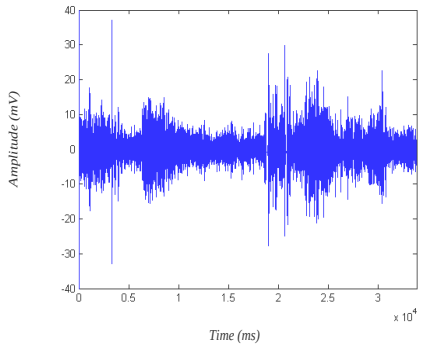

Fig 12: Noisy signal spectrum after filtering in the time domain

It can be seen that the filtering allows for clear distinction between the two signal types, where the amplitude is much lower in the clean signal. From experiments we made it turns out that the values changes slightly depending on the light intensity and the environmental noise. That brought us to a conclusion to make calibration before using the system. During the use of the system, in the background, a comparison between the values obtained after filtering and the maximum value obtained during calibration will be performed. In case of values that are bigger than the maximum value, the system will produce a message that the signal is noisy.

A. Filtering the EOG signal of A/D board

After the success we had in filtering and distinguishing between the clean and noisy signal we returned to the A/D board and tested manipulations directly on the digital words that come out from the A/D board. We created an entity named signal_process that will serve the system in the filtering operation. The process transferred the digital words at the output of the A/D to the RS-232 output. Then, a connection between the RS-232 output ton the computer COM port was made. The sampling rate that still allowed for reliable communication was 350Hz. Since the signal goes through low pass filter with cutoff frequency of 50Hz, sampling rate of 350Hz is more than required according to Nyquist-Shannon sampling theorem. Figures 13 and 14 present the clean signal received after sampling of the A/D output in both time and frequency domains respectively. Figure 15 presents the noisy signal received after sampling of the A/D output in frequency domain.

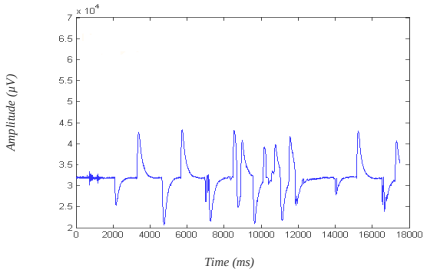

Fig 13: Clean signal in the time domain

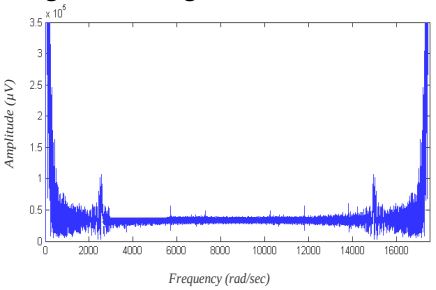

Fig 14: Clean signal spectrum in the frequency domain

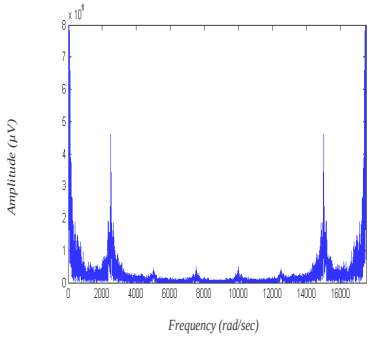

Fig 15: Noisy signal spectrum in the frequency domain

V. RESULTS ANALYSIS

The spectrum seems to be identical to the sampling spectrum taken directly from the LABchart, except for the fact that the frequency components are more powerful. That stems from the fact that the A/D input is the signal at the output of the BIO-AMP, which is the amplification of the voltages measured from the eyes, and the samples presented in LABchart shown in their actual order which is much smaller. 2. Here we can see peaks around 50Hz as well, just that in comparison to the previous spectrum figures it is received in higher frequency of the discrete signal spectrum. The reason for that is that the sampling frequency is smaller (350Hz vs. 1KHz), which cause for spectrum spreading.

A. Design of the FIR filter

Linear phase is not required here, so we used Laplace transform for the filter design. The noised signal is composed of a dc component and a different amplitude noise signals. Eq. 2 presents the required band pass filter transfer function

ISSN: 2277-3754
ISO 9001:2008 Certified
International Journal of Engineering and Innovative Technology (IJEIT)
Volume 4, Issue 3, September 2014

$$\frac{s+a}{(s+b)(s+c)} = \frac{A}{s+b} + \frac{B}{s+c} \quad (2)$$

Where a,b, and c are frequencies of a zero and two poles respectively. The right hand side of Eq. 2 is the partial fraction shape of the left side.

Solving Eq. 2 for A and B gives:

$$A = \frac{b-a}{c-a} \; ; \; B = \frac{c-b}{c-a} \quad (3)$$

In addition, *A* and *B* keep the condition shown in Eq. 4:

$$A + B = 1 \quad (4)$$

The reversed Laplace transform will take the form presented in Eq. 5:

$$Ae^{-bt} + Be^{-ct} \quad (5)$$

Substituting *t=KT* for discrete time domain results in Eq. 6:

$$\sum_{K=1}^{\infty} Ae^{-bKT} + \sum_{K=1}^{\infty} Be^{-cKT} \quad (6)$$

Next step is applying Z Transform to Eq. 6 taking into account equations 3 and 4 will yield Eq. 7 and Eq. 8:

$$\sum_{K=0}^{\infty} Ae^{-bKT}Z^{-K} = \frac{A}{1-e^{-bT}Z^{-1}} = A + Ae^{-bT}Z^{-1} + \cdots + Ae^{-bKT}Z^{-K} \quad (7)$$

$$\sum_{K=0}^{\infty} Be^{-cKT}Z^{-K} = \frac{B}{1-e^{-cT}Z^{-1}} = B + Be^{-cT}Z^{-1} + \cdots + Be^{-cKT}Z^{-K} \quad (8)$$

Then, summing the two expressions of Eq. 7 and Eq. 8 will produce Eq. 9:

$$\sum_{K=0}^{\infty} Ae^{-bKT}Z^{-K} + \sum_{K=0}^{\infty} Be^{-cKT}Z^{-K} = A + B + Ae^{-bT}Z^{-1} + Be^{-cT}Z^{-1} + \cdots + Ae^{-bKT}Z^{-K} + Be^{-cKT}Z^{-K} \quad (9)$$

Applying inverse Z transform to Eq. 9 for difference equation will produce Eq. 10:

$$f(t) = 1\delta[t] + (Ae^{-bT} + Be^{-cT})\delta[t-1] + \cdots + (Ae^{-bKT} + Be^{-cKT})\delta[t-K] \quad (10)$$

The coefficients obtained from Eq. 10 are presented in Eq. 11:

$$1, \; Ae^{-bT} + Be^{-cT}, \; Ae^{-b2T} + Be^{-c2T}, \; \vdots, \; Ae^{-bKT} + Be^{-cKT} \quad (11)$$

As before, the most significant difference between the amplitudes of the two signals occurred in frequencies between 60Hz and 80Hz. According to that, we designed a FIR band pass filter with 150 coefficients (Eq. 11) for the purpose of signal filtering. Figure 16 presents the image of the filter in the frequency domain. In the time domain, FIR filters are typically truncated and time shifted SINC. Figure 17 presents the image of the filter in the time domain.

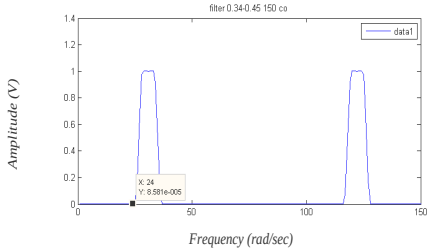

Fig 16: Frequency domain of the FIR band pass filter

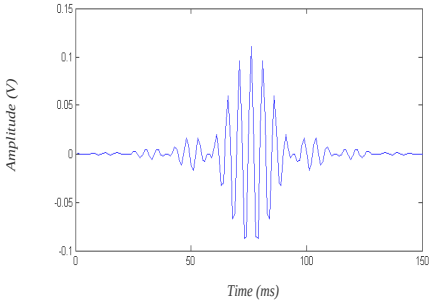

Fig 17: Time domain of the FIR band pass filter

Figures 18 and 19 present the spectrum of the clean signal and the noisy signal after filtration respectively. It can be seen that the frequency amplitude difference is definitely significant.

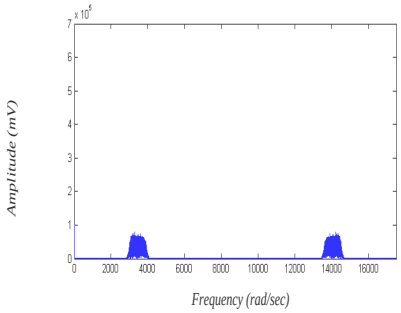

Fig 18: Clean signal spectrum after filtering

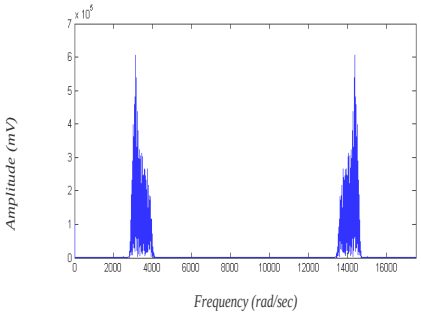

Fig 19: Noisy signal spectrum after filtering

In the time domain the amplitude difference is significant as well as can be seen in figures 20 and 21.

ISSN: 2277-3754
ISO 9001:2008 Certified
International Journal of Engineering and Innovative Technology (IJEIT)
Volume 4, Issue 3, September 2014

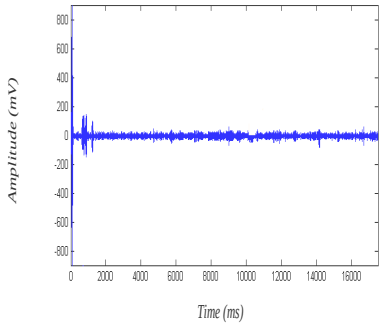

Fig 20: Clean signal in time domain

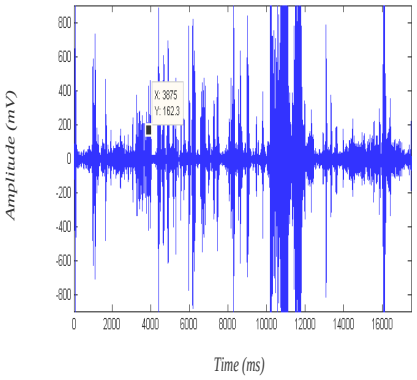

Fig 21: Noisy signal in time domain

The next step was to implement the FIR filter in VHDL language and burn it into the Xilinx fpga within the ADC board. We used the Xilinx FIR generator called FIR core in order to realize the filter. Figure 22 presents the filter specifications with the coefficients that we fed according to the MatLab coefficients we received earlier. In this case the clock frequency and sampling frequency were both 350Hz, input signal data width was 16 bit, unsigned. Figure 22 presents a summary of the FIR filter specifications.

Fig 22: FIR core specification

The frequency response of the filter (in dB) is presented in figure23. This frequency response is compatible to what was received from MatLab.

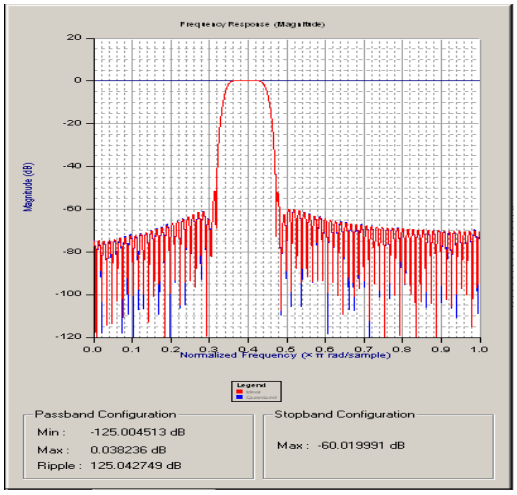

Fig 23: FIR frequency response in dB

B. Adaptation of the FIR filter to the FPGA board

It turned out that the design of a filter with 150 coefficients was too big for the Xilinx board. We had to reduce the number of coefficients to 15 for the FIR filter (in addition to a LPF filter with 15 coefficients as well). Tests we performed with the same cut-off frequencies showed that the FIR filters low frequencies significantly bad, so we reduced the transfer range and shifted the range towards the higher frequencies. The new filter spectrum is presented in figure 24.

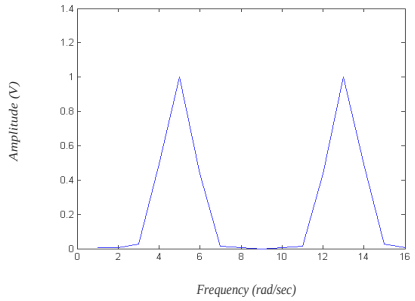

Fig 24: New filter spectrum

In order to demonstrate the new filter operation, we will present mixed signal of clean signal followed by a noisy signal in time domain as appears in figure 25. The output of the filter is presented in figure 26.

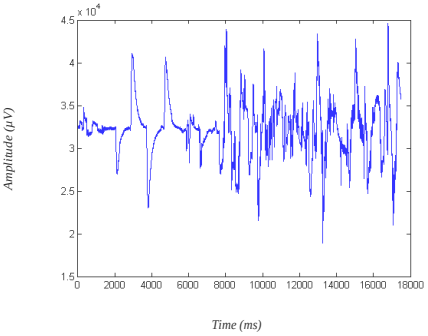

Fig 25: Mixed signal input to the new filter

ISSN: 2277-3754
ISO 9001:2008 Certified
International Journal of Engineering and Innovative Technology (IJEIT)
Volume 4, Issue 3, September 2014

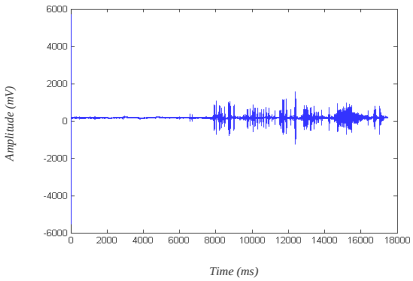

Fig 26: Mixed signal after filtration

It can be seen from figure 26 that the amplitude of the signal during the time of the noisy signal is relatively high in relation to the amplitude of the signal during the time of the clean signal. In addition to this selector filter, we added a LPF filter for environmental noise filtration, as appear in the literature. The filter detected energy levels for a clear distinction between the signal and the noise. It also helped with the user interface. In order to operate the robotic manipulator, the user was asked to perform three eye movements, when after each movement the user confirm the movement by looking to the center for five seconds. The use of the LPF reduced significantly the noises appeared during staring to the center. Figure 27 presents the LPF filtering of a mixed signal. It is smoother than the signals received before the filtration. The filter has 15 coefficients due to hardware constraints

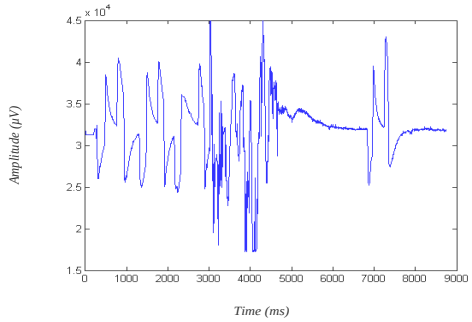

Fig 27: Mixed signal LPF filtration

The filter image in the frequency domain is presented in figure 28. Figure 29 presents the filter image in frequency domain with zeros 'quilting'.

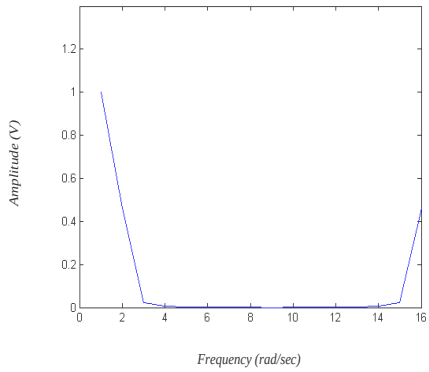

Fig 28: The filter image in the frequency domain

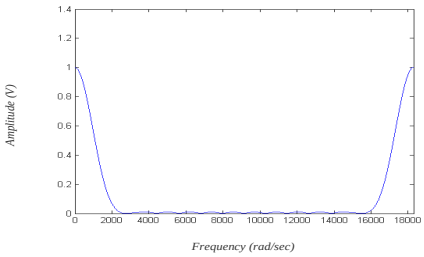

Fig 29: The filter image in frequency domain with zeros 'quilting.

VI. MANIPULATOR OPERATION

The manipulator used for this research was of Lynxmotion and is shown in figure 30.

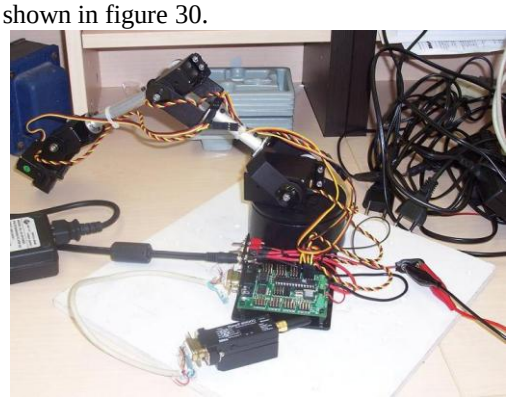

Fig 30: The manipulator with 5 DOF and gripper

The robot features: base rotation, single plane shoulder, elbow, wrist motion, wrist rotation, and a functional gripper. The arm uses 1 x HS-475HB in the base, 1 x HS-5745MG in the shoulder, 1 x HS-5745MG in the elbow, 1 x HS-645MG in the wrist, wrist rotation uses 1 x HS-85BB and 1 x HS-422 in the gripper. The manipulator comes with RIOS (Robotic arm Interactive Operating System) for controlling the robotic arms with the SSC-32 servo controller. The inverse kinematics engine helps in positioning the arm accurately. The servo motors were controlled from the fpga board. The force gripper sensing resistor output that is proportional to the amount of force applied, helped in designing the closing and openning of the gripper. Each command, like "Move to the right 20 units" was implemented after 3 successful successive eye movements (see figure 31). Then the program translated it to a series of servo commands in the form of #<ch>P<pw>, where <ch> stands for servo number and <pw> stands for pulse width. The pulse width modulation was locked anti-phase such that pulse width data includes both desired direction and angle data. Figure 31 presents the arm state machine for the complete operation of the manipulator.

VII. CONCLUSION AND DISCUSSION

A real time accurate, reliable, and robust EOG signal processing device without use of a video camera has been designed, built and implemented. The used method allowed for controlling a manipulator with only eye movement of a

ISSN: 2277-3754
ISO 9001:2008 Certified
International Journal of Engineering and Innovative Technology (IJEIT)
Volume 4, Issue 3, September 2014

severely disabled person that lost motor functionality and is capable of eye movements only. A novel analysis of the EOG signal was introduced. Greater reliability of the system was assured with further reduction of noises coming from other physiological signals like EEG and EOG. Manipulator commands were coded into three eye movements each. Horizontal eye movements were distracted from each eye movement and were fed into the logic control engine. This system can be used in other applications like spell and speak using common software packages, paint, etc.

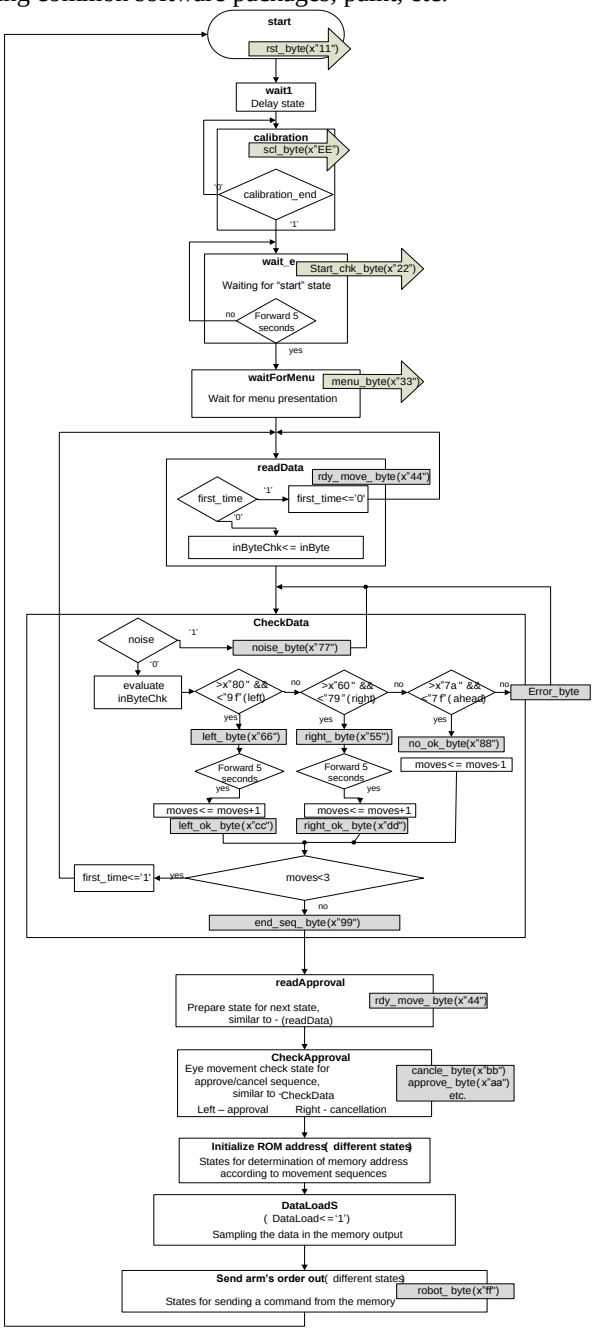

Fig 31: The manipulator algorithmic state machine

VIII. ACKNOWLEDGMENT

The authors thank Liron Fortgang and Chaim Charazi for their contributions to the research.

REFERENCES

[1] http://www.nationalmssociety.org/about-multiple-sclerosis/what-we-know-about-ms/FAQs-about-MS/index.aspx#howmany.

[2] Valencia P. Higuera, Multiple Sclerosis: Affecting 2.5 Million Worldwide. GoogoBits, 2005, http://www.googobits.com/articles/p0-2278-multiple-sclerosis-affecting-25-million-worldwide.html.

[3] http://www.ninds.nih.gov/disorders/amyotrophiclateralsclerosis/detail_amyotrophiclateralsclerosis.htm.

[4] O. Ji and Z. Zhu, "Eye and gaze tracking for interactive graphic display," Mach. Vis. Appl., vol. 15, no. 3, pp. 139–148, Jul. 2004.

[5] K. R. Park, "A real-time gaze position estimation method based on a 3-D eye model," IEEE Trans. Syst., Man, Cybern. B, Cybern., vol. 37, no. 1, pp. 199–212, Feb. 2007.

[6] D. W. Hansen and A. E. C. Pece, "Eye tracking in the wild," Comput. Vis.Image Underst., vol. 98, no. 1, pp. 155–181, Apr. 2005.

[7] S. Kawato and N. Tetsutani, "Detection and tracking of eyes for gazecamera control," Image Vis. Comput., vol. 22, no. 12, pp. 1031–1038, Oct. 2004.

[8] John J. Magee, Margrit Betke, James Gips, Matthew R. Scott, and Benjamin N. Waber, A Human–Computer Interface Using Symmetry Between Eyes to Detect Gaze Direction, IEEE Trans. On Sys., Man, and Cybernetics –Part A: Systems and Humans, vol. 38, no. 6, Nov. 2008, , pp. 1248-1261.

[9] D. Kumar, and E. Poole, Classification of EOG for Human Computer Interface, Proc. Of the sec joint EMBS/BMES Conf. Houston, Tx, USA, Oct. 2002, pp. 64-67.

[10] S. R. Choudhury, S.Venkataramanan, H. B. Nemade, J.S. Sahambi, Design and Development of a Novel EOG Biopotential Amplifier, IJBEM, vol 7, no. 1, pp. 271-274, 2005.

[11] B. R. Greene φ, S. Meredith, R. B. Reilly and G. Donohoe, A novel, portable eye tracking system for use in Schizophrenia Research, ISSC 2004, Belfast, June 30 - July 2, 2004.